



CAB models for water: A new evaluation of the thermal neutron scattering laws for light and heavy water in ENDF-6 format



J.I. Márquez Damián^{a,*}, J.R. Granada^a, D.C. Malaspina^b

^a Neutron Physics Department and Instituto Balseiro, Centro Atómico Bariloche, CNEA, Argentina

^b Department of Biomedical Engineering and Chemistry of Life Processes Institute, Northwestern University, 2145 Sheridan Road, Evanston, IL 60208, United States

ARTICLE INFO

Article history:

Received 29 August 2013

Received in revised form 5 November 2013

Accepted 7 November 2013

Available online 6 December 2013

Keywords:

Light water

Heavy water

Thermal neutron scattering

Scattering law

NJOY

ENDF-6

ABSTRACT

In this work we present the *CAB models for water*: a set of new models for the evaluation of the thermal neutron scattering laws for light and heavy water in ENDF-6 format, using the LEAPR module of NJOY. These models are based on experimental structure data and frequency spectra computed from molecular dynamics simulations. The calculations show a significant improvement over ENDF/B-VI and ENDF/B-VII when compared with measurements of differential and integral scattering data.

© 2013 Elsevier Ltd. All rights reserved.

1. Introduction

Light and heavy water are the moderators more commonly used in nuclear reactors. These substances have been extensively studied with theoretical and experimental methods, both to understand their anomalous physicochemical properties and to model the interaction of neutrons with them. Despite these efforts, the thermal scattering data available to the users from the evaluated data libraries come from essentially two different models (MacFarlane, 1994; Mattes and Keinert, 2005), which are both based on experimental data measured in the 1960s.

Since then, there have been important advances in the study of structure and dynamics of water both with theory and experiments. Among the experiments it is important to highlight structure determinations from diffraction measurements by Dore (1985), Walford et al. (1977) and Soper and Benmore (2008), and the measurements of the dynamics by Bellissent-Funel et al. (1995), Teixeira et al. (1985) and Novikov et al. (1990) using quasi-elastic and double differential spectrometers. On the theoretical side there have been important advances on molecular dynamics simulations, from the seminal work by Rahman and Stillinger (1971), to the extensive simulations by Marti et al. (1996) and the flexible four-site model TIP4P/2005f by González and Abascal (2011).

During the last few years we have been working (Marquez Damián et al., 2011; Viñales et al., 2011; Marquez Damián et al., 2013) at the Neutron Physics Department at Centro Atómico Bariloche on a review of the existing models for the calculation of the thermal scattering laws for light and heavy water, building upon the important advances of these last decades and motivated by similar, but independent, work on molecular dynamics by Abe et al. (2014). As a result of this effort, we present in this paper the *CAB models for water*, a series of thermal neutron scattering models for light and heavy water that are based on both experimental data and molecular dynamics simulations, and the methodology to generate them at the desired temperature. Molecular dynamics is used to obtain the generalized frequency spectrum whereas experimental data from Novikov is used to estimate the diffusive mass. Partial structure factors, determined experimentally by Soper, are used to calculate the coherent scattering component in heavy water.

2. Thermal scattering files

The double differential thermal scattering cross section for neutrons with incident energy E , secondary energy E' and scattering angle θ on a material with bound scattering cross section σ_b and mass Am_n at temperature T can be written as:

$$\frac{d^2\sigma}{d\Omega dE} = \frac{\sigma_b}{4\pi kT} \sqrt{\frac{E'}{E}} S(\alpha, \beta) \quad (1)$$

* Corresponding author. Tel.: +54 2944445216.

E-mail address: marquezj@cab.cnea.gov.ar (J.I. Márquez Damián).

where $S(\alpha, \beta)$, the scattering law, is a function of the adimensionalized change in momentum:

$$\alpha = \frac{E + E' - 2\sqrt{EE'} \cos \theta}{AkT} \quad (2)$$

and change in energy:

$$\beta = \frac{E' - E}{kT} \quad (3)$$

Thermal scattering law files for nuclear engineering applications are now commonly distributed in the ENDF-6 format (Herman and Trkov, 2009) as MF = 7, for materials on which the free gas approximation is not sufficient.

3. Existing models

The thermal scattering law files are produced from physical models, which are sets of parameters that define the dynamics and structure of the scatterer within the theoretical framework of the processing programs. To this day, all the thermal scattering files for light and heavy water distributed in the major evaluated nuclear data libraries (Table 1) for reactor calculations were produced with only two essentially different models: one was prepared by the General Atomics group (from now on, the GA model) in the 1960s, and the other was initially proposed by Keinert and Mattes at IKE Stuttgart in the 1980s and updated in the mid 2000s (from now on, the IKE model).

3.1. GA models

The GA models for light and heavy water (Table 2) were initially compiled by Koppel and Houston (1978). These models were processed using GASKET (Koppel et al., 1967), and the resulting scattering law files were included in the ENDF/B-III thermal scattering library. In 1994, MacFarlane adapted the light water model to be used with the LEAPR module of NJOY and included the resulting file in the ENDF/B-VI thermal scattering library (MacFarlane, 1994). The file for heavy water was converted to ENDF-6 format and included in the library.

The model for light water includes only the scattering for H in H₂O, and oxygen is represented as a free gas with mass 16. This

Table 2
Parameters for the General Atomics Models.

	H ₂ O	D ₂ O
Translational weight (w_t)	1/18	2/40
Continuous spectrum weight (w_c)	0.444	0.450
First osc. energy (E_{v_2}) (meV)	205	142
First osc. weight (w_{v_2})	0.166	0.166
Second osc. energy ($E_{v_{1,3}}$) (meV)	480	305
Second osc. weight ($w_{v_{1,3}}$)	0.333	0.333

Table 3
Parameters for the IKE models at 293 K.

	H ₂ O	D ₂ O
Translational weight (w_t)	1/46	2/40
Continuous spectrum weight (w_c)	0.478	0.450
First osc. energy (E_{v_2}) (meV)	205	145
First osc. weight (w_{v_2})	0.166	0.166
Second osc. energy ($E_{v_{1,3}}$) (meV)	436	338
Second osc. weight ($w_{v_{1,3}}$)	0.333	0.333

model is based on a continuous frequency spectrum obtained by Haywood and Thorson (1962) which is used to represent the hindered rotations. The low energy part of the spectrum is replaced by a ω^2 function and the translation of the molecule is represented as a free gas with mass 18. Two discrete oscillators are included to model the internal vibration: one at $E_{v_2} = 205$ meV represents the scissoring mode and another at $E_{v_{1,3}} = 480$ meV is used to represent the symmetric and asymmetric stretching modes.

Despite the preponderance of coherent scattering in deuterium and oxygen, the GA model for heavy water was computed using the incoherent approximation implemented in GASKET. For thermalization applications Koppel and Young (1965) showed that the effects of coherence are of second order, although the resulting differential and total cross sections might differ appreciably from measured values.

The model for heavy water is a model for D in D₂O, and oxygen is treated as a free gas with mass 16. A continuous frequency spectrum based on data by Haywood and Thorson is used to describe the hindered rotations. Below 25 meV the spectrum is replaced by ω^2 , and the translation of the molecule is represented as a free

Table 1
Scattering law files available from major evaluated nuclear data libraries.

Library	Model	Comments
ENDF/B-VI.8 (USA, 2002)		
H (H ₂ O)	GA	Evaluated in 1969 by Koppel and Young with GASKET. Modified in 1994 by MacFarlane to run in LEAPR
D (D ₂ O)	GA	Evaluated in 1969 by Koppel and Young with GASKET. Adapted in 1989 to ENDF-6 format
JEFF 3.1.1 (Europe, 2009)		
H (H ₂ O)	IKE	Evaluated by Keinert and Mattes in 2004 with LEAPR
D (D ₂ O)	IKE	Evaluated by Keinert and Mattes in 2004 with LEAPR
ENDF/B-VII.1 (USA, 2011)		
H (H ₂ O)	IKE	Adapted by MacFarlane in 2006
D (D ₂ O)	IKE	Adapted by MacFarlane in 2006
JENDL 4.0 (Japan, 2010)		
H (H ₂ O)	GA	Data taken from ENDF/B-VI.8
D (D ₂ O)	GA	Data taken from ENDF/B-VI.8
RUSFOND-2010 (Russia, 2010)		
H (H ₂ O)	IKE	Data taken from ENDF/B-VIIIb2
D (D ₂ O)	IKE	Data taken from ENDF/B-VIIIb2
CENDL 3.1 (China, 2009)	–	Thermal scattering library not included.
BROND 2.2 (Russia, 1993)	–	Thermal scattering library not included.
TENDL-2012 (Europe, 2012)	–	Thermal scattering library not included.

gas with mass 40. Two discrete oscillators are included in the model to represent internal vibrations: one at $E_{v_2} = 142$ meV (scissoring mode) and another at $E_{v_{1,3}} = 305$ meV (stretching modes).

3.2. IKE models

The IKE models for light and heavy water (Table 3) were originally proposed by Keinert and Mattes at IKE Stuttgart in 1984, and the resulting scattering law files were adopted for the JEF-1 thermal scattering library (Keinert et al., 1984). The models were originally processed with GASKET.

In 2003 work started at IKE to update the thermal scattering models using LEAPR as the processing tool. The resulting models were published by Mattes and Keinert (2005) and were later adapted by MacFarlane and included in the ENDF/B-VII thermal scattering library (Chadwick et al., 2011).

The model for light water is a model for H in H₂O and oxygen is treated as a free gas with mass 16. The rotational band is temperature dependent, and is interpolated from the measurements by Haywood and Page at 300 and 550 K (Haywood and Page, 1968). The collective intermolecular modes of the spectrum are replaced by a ω^2 function, and the translational mode is represented as a free gas with temperature-dependent mass to model molecular clusters. The internal modes are represented as discrete oscillators with $E_{v_2} = 205$ meV, $E_{v_{1,3}} = 435$ meV.

The model for heavy water is a model for D in D₂O, and oxygen is treated as a free gas with mass 16. A continuous spectrum, adapted from measurements by Haywood and Page at 300 K and 550 K is used to represent the hindered rotations and intermolecular vibrations, the later being included as a Debye spectrum with $kT_D = 20.2$ meV. The internal vibration modes are represented as discrete oscillators with $E_{v_2} = 145$ meV, $E_{v_{1,3}} = 338$ meV. Coherent scattering from deuterium is considered using the Sköld approximation, with a structure factor computed from a Lennard–Jones model.

4. Proposed models: CAB models for water

4.1. Calculation of the frequency spectra

When the scattering law is computed in the Gaussian approximation, the key parameter needed to define the dynamics is the frequency spectrum. In our models, the frequency spectra are obtained from molecular dynamics simulations. The procedure to obtain the frequency spectrum is briefly explained here, and further details can be found in reference (Marquez Damian et al., 2013).

A system of 512 molecules of TIP4P/2005f water (González and Abascal, 2011) is modeled in GROMACS (Van Der Spoel et al., 2005), for a simulation time of 100 ps with a timestep of 0.1 fs at constant pressure and temperature. From the resulting trajectory file, containing the velocity of each particle for frames each 0.6 fs, the velocity autocorrelation function (VACF) is extracted:

$$\text{VACF}_x(\tau) = \langle v_x(t) \cdot v_x(t + \tau) \rangle$$

Here, $\langle \cdot \rangle$ is the ensemble average over a particular group of atoms (D, H, O).

Using these results, frequency spectra is computed as the cosine Fourier transform of the VACF:

$$\rho(\epsilon) = \frac{M}{3\pi kT} \frac{1}{2\pi} \int_0^\infty \text{VACF}(\tau) \cos(\omega\tau) d\tau$$

where $\epsilon = E' - E = \hbar\omega$ is the excitation energy.

This procedure is summarized in Fig. 1.

As an example of this process, the generalized frequency spectrum for H in H₂O at 300 K is shown in Fig. 2. The calculation is

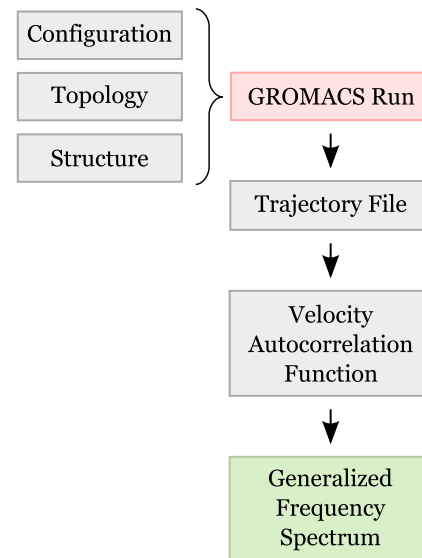


Fig. 1. Generalized frequency spectra calculation process.

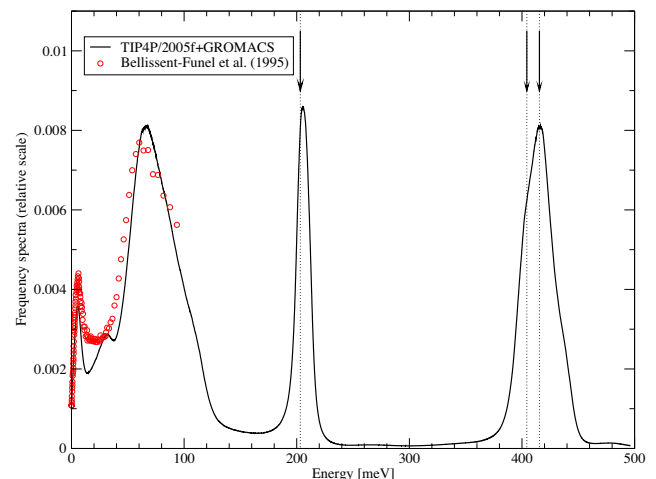


Fig. 2. Generalized frequency spectrum for H in H₂O at 300 K.

compared with neutron scattering measurements by Bellissent-Funel et al. (1995), and normal mode energies measured by Lappi et al. (2004) by infrared spectroscopy (marked with arrows).

4.2. LEAPR models

4.2.1. Light water

The model for light water is a model for H in H₂O, computed in the incoherent approximation, whereas oxygen is treated as a free gas with mass 16. The model is composed of three components that are convoluted:

1. Molecular diffusion, represented with the Egelstaff–Schofield model.
2. Intermolecular stretching and bending of the hydrogen bond network and molecular librations, represented as a continuous spectrum.
3. Internal vibrations, represented as discrete oscillators.

Starting from the generalized frequency spectrum computed from molecular dynamics at the corresponding temperature, the continuous spectrum is obtained by subtracting modes.

$$\rho_{\text{cont}}(\epsilon) = \rho(\epsilon) - \rho_{\text{diff}}(\epsilon) \quad (\text{for } \epsilon < 158 \text{ meV}) \quad (4)$$

The diffusion component of the spectrum is represented using the Egelstaff–Schofield expression for the diffusive frequency spectrum (Egelstaff and Schofield, 1962):

$$\rho_{\text{diff}}(\epsilon) = \frac{4cw_t}{\pi\hbar kT} \sqrt{c^2 + 1/4} \cdot \sinh(\epsilon/(2kT)) \cdot K_1 \left\{ \epsilon/(kT) \sqrt{c^2 + 1/4} \right\} \quad (5)$$

where c is a non-dimensional diffusion constant:

$$c = \frac{M_{\text{diff}}D}{\hbar} = \frac{M_{\text{H}}D}{w_t\hbar} \quad (6)$$

and w_t is the translational weight:

$$w_t = \frac{M_{\text{H}}}{M_{\text{diff}}} \quad (7)$$

To compute these parameters we need the diffusion coefficient and the diffusion mass. The diffusion coefficient is obtained from the generalized frequency distribution:

$$\lim_{\epsilon \rightarrow 0} \rho(\epsilon) = \frac{2m_{\text{H}}D}{\pi\hbar} \Rightarrow D = \frac{\pi\hbar\rho(0)}{2m_{\text{H}}} \quad (8)$$

In Fig. 3 we show an Arrhenius plot of the diffusion coefficient computed with Eq. (8) from molecular dynamics simulations with the TIP4P/2005f, compared with measurements by Mills (1973) and Yoshida et al. (2005).

In the generalized frequency spectrum produced from molecular dynamics, the diffusion component is combined with the rest of the dynamical modes, and the diffusion mass cannot be always extracted. For this reason, in our calculation we estimate the diffusion mass from the measurements by Novikov et al. (1990) (Table 4).

Finally, the weight corresponding to internal vibrations is integrated from the generalized frequency spectrum above 158 meV, and distributed equally in one bending mode at 205 meV and two degenerate stretching modes at 430 meV. The remaining continuous spectrum is adjusted to approach $\omega = 0$ as ω^2 to ensure the convergence of the phonon approximation used in LEAPR.

The parameters calculated for 300 K are listed in Table 5 and the continuous frequency spectrum is shown in Fig. 4.

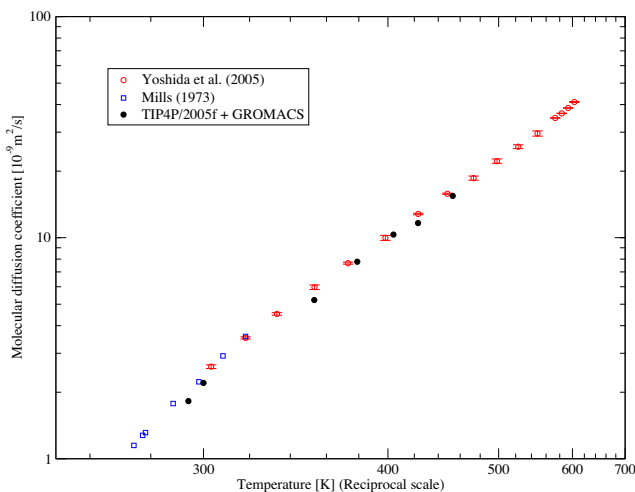


Fig. 3. Arrhenius plot of the molecular diffusion coefficient for light water.

Table 4

Diffusion masses for light water, from measurements by Novikov et al. (1990).

T [K]	$m_{\text{diff}}/m_{\text{H}_2\text{O}}$
300	6.49
400	2.10
500	2.25
600	1.44

Table 5

Parameters for the CAB models at 300 K.

	H ₂ O	D(D ₂ O)	O(D ₂ O)
Translational weight (w_t)	0.008605	0.015475	0.122896
Diffusion constant (c)	4.060575	4.098718	3.720393
Continuous spectrum weight (w_c)	0.522421	0.541899	0.725760
First osc. energy (E_{v_2}) (meV)	0.205	0.145	0.145
First osc. weight (w_{v_2})	0.156325	0.147542	0.050448
Second osc. energy ($E_{v_{1,3}}$) (meV)	0.430	0.303	0.303
Second osc. weight ($w_{v_{1,3}}$)	0.312649	0.295084	0.100896

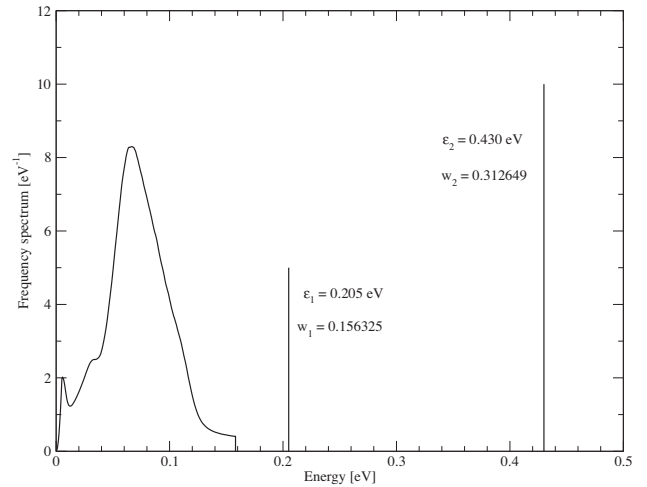


Fig. 4. Continuous frequency spectrum for H in H₂O at 300 K.

4.2.2. Heavy water

In the case of heavy water, it was found that oxygen cannot be treated as free gas. For that reason, the model includes components for D in D₂O and O in D₂O.

Starting from a molecular dynamics simulation for D₂O at each specific temperature and pressure, the autocorrelation function and the generalized frequency spectrum for the velocities of deuterium and oxygen were computed. Each model is prepared from the corresponding generalized frequency spectrum, and has the same components as the model for H in H₂O:

1. Molecular diffusion, represented with the Egelstaff–Schofield model.
2. Intermolecular stretching and bending of the hydrogen bond network and librations, represented as a continuous spectrum.
3. Internal vibrations, represented as discrete oscillators.

Again, the continuous spectrum is obtained by subtracting the Egelstaff–Schofield diffusion spectrum and the contribution of the internal vibration modes:

$$\rho_{\text{cont}}(\epsilon) = \rho(\epsilon) - \rho_{\text{diff}}(\epsilon) \quad (\text{for } \epsilon < 120 \text{ meV}) \quad (9)$$

The diffusion coefficient is calculated from $\rho(0)$, and the diffusion mass is computed assuming the same molecular cluster size as observed by Novikov in light water. E.g. for 300 K:

$$m_{\text{diff}}^{\text{H}_2\text{O}} = 6.49 m_{\text{H}_2\text{O}} \quad (10)$$

$$m_{\text{diff}}^{\text{D}_2\text{O}} = 6.49 m_{\text{D}_2\text{O}} \quad (11)$$

The parameters calculated for 300 K are listed in Table 5 and the continuous frequency spectrum is shown in Fig. 5.

The coherent component is computed using the Sköld approximation:

$$S(\alpha, \beta) = S_{\text{inc}}(\alpha, \beta) + S_{\text{coh}}(\alpha, \beta) \quad (12)$$

$$S_{\text{coh}}^D(\alpha, \beta) = S_{\text{inc}}^D(\alpha/\tilde{S}^D(Q), \beta)\tilde{S}^D(Q) \quad (13)$$

$$S_{\text{coh}}^O(\alpha, \beta) = S_{\text{inc}}^O(\alpha/\tilde{S}^O(Q), \beta)\tilde{S}^O(Q) \quad (14)$$

where $\tilde{S}^D(Q)$, $\tilde{S}^O(Q)$ are the Sköld correction factors for deuterium and oxygen:

$$\tilde{S}^D(Q) = 1 + \frac{2}{3} [S_{\text{DD}}(Q) - 1] + \frac{1}{3} \frac{b_{\text{coh}}^O}{b_{\text{coh}}^D} [S_{\text{DO}}(Q) - 1] \quad (15)$$

$$\tilde{S}^O(Q) = 1 + \frac{2}{3} [S_{\text{OO}}(Q) - 1] + \frac{1}{3} \frac{b_{\text{coh}}^D}{b_{\text{coh}}^O} [S_{\text{DO}}(Q) - 1] \quad (16)$$

Here, $S_{ij}(Q) = S_{\text{Do}}(Q), S_{\text{Do}}(Q), S_{\text{DD}}(Q)$ are the partial structure factors of heavy water, obtained by Soper and Benmore (2008). The correction factors are computed in the polyatomic approximation proposed by Vineyard (1958), which approximates the real molecular structure of the liquid.

The Sköld correction factors for deuterium and oxygen in D_2O at 300 K are shown in Fig. 6.

5. Results and validation

In this section we compare calculations with our model, ENDF/B-VI, and ENDF/B-VII with experimental values. Unless explicitly noted, the calculations are performed at room temperature.

It is important to note that all the constants in the thermal scattering models were extracted either from molecular dynamics simulations or from experimental data, and none of the calculations presented in this section result from the adjustment of free parameters.

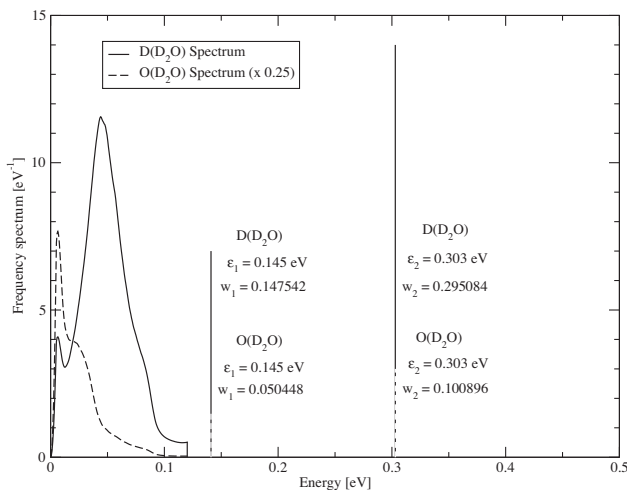


Fig. 5. Continuous frequency spectrum for D and O in D_2O at 300 K.

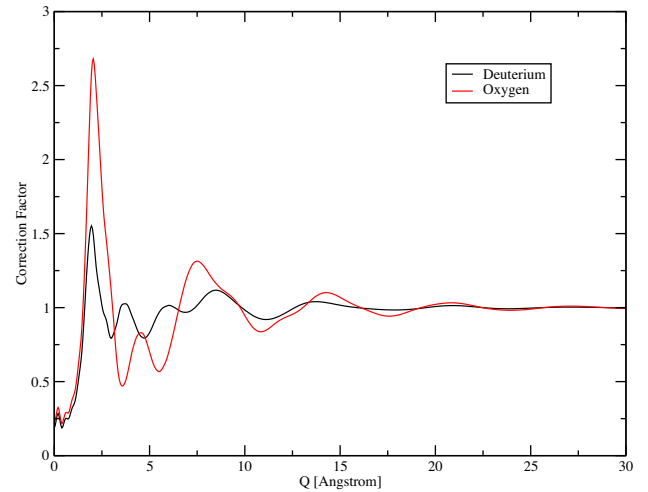


Fig. 6. Sköld correction factors for deuterium and oxygen in D_2O at 300 K.

5.1. Double differential scattering cross section

The double differential scattering cross section for light and heavy water were computed from the scattering law files using the ENDF-reading capabilities of the PYNE library (Scopatz et al., 2012) and compared with different series of experimental data.

Bischoff et al. (1967) published a series of measurements of the double differential scattering cross section for light water, performed at the Rensselaer Polytechnic Institute neutron scattering system, based on the RPI LINAC. The energy resolution of the instrument was not published with the data, but from low angle scattering experiments it is estimated to be $\Delta E_0/E_0 \sim 5\%$. The low energy resolution and high experimental uncertainty of these experiments makes them a not very strict test of the cross sections. Overall, both results computed with ENDF/B-VII and our model show a similar qualitative behavior. As an example, in Fig. 7 we show a comparison for $E_0 = 154$ meV and $\theta = 14^\circ$.

Novikov et al. (1986) measured the double differential cross section of light water using the DIN-1M spectrometer of the IBR reactor in Dubna. The incident energy used was 8 meV with a resolution of 0.57 meV. The comparison with calculated results shows (Fig. 8) a clear improvement when the new model is used, caused

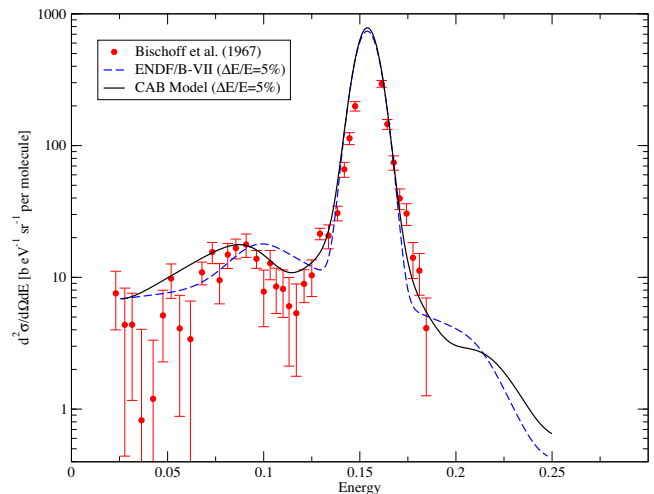


Fig. 7. Double differential scattering cross section for light water, $E_0 = 154$ meV, $\theta = 14^\circ$.

mainly by the replacement of free gas dynamics by diffusion. This effect can be seen in more detail when the calculations are compared with quasielastic scattering measurements.

In the case of heavy water, we compared our calculation with the measurements by Harling (1968), who published a series of scattering measurements on water performed at the Battelle Rotating Crystal Spectrometer. The incident energies used were 101 meV and 213 meV with a resolution $\approx 6\%$ for the lower incident energy. When ENDF/B-VII and the new model are compared with these experimental results an overall better agreement is found for all angles. As an example, in Fig. 9 we show the results for $E_0 = 101$ meV, $\theta = 60^\circ$.

5.2. Quasi-elastic scattering

A more strict test for low energy dynamics is the comparison with measurements of the double differential cross section under low energy exchange, or quasi-elastic, conditions. In Fig. 10 we compare measurements published by Bellissent-Funel (1984) of the double differential cross section of light water for $E_0 = 2.35$ meV, $\theta = 64.20^\circ$ with calculations using our model and ENDF/B-VII. There is a clear difference between the width of the quasielastic peaks computed using both models.

Quasi-elastic scattering results are typically represented as energy widths or half-widths plotted as a function of the square of momentum change. The scattering law for a system that follows the Fick’s diffusion law has a Lorentzian shape (Egelstaff, 1967):

$$S(Q, \omega) = \frac{1}{\pi} \frac{DQ^2}{\omega^2 + (DQ^2)^2} \tag{17}$$

Then, the half-width at half maximum of the double differential cross section at measured constant Q is DQ^2 . This also holds for other simple diffusion models, like the Egelstaff–Schofield diffusion model.

If we compare (Fig. 11) the half-width at half maximum of the quasielastic peak calculated at 293 K with our model with measurements by Teixeira et al. (1985) we can observe our model predicts a DQ^2 behavior, departing from the measurements at high Q . If this difference is important, the scattering law can be computed directly from molecular dynamics simulations. Still, the overall behavior of the model is a clear improvement over ENDF/B-VII.

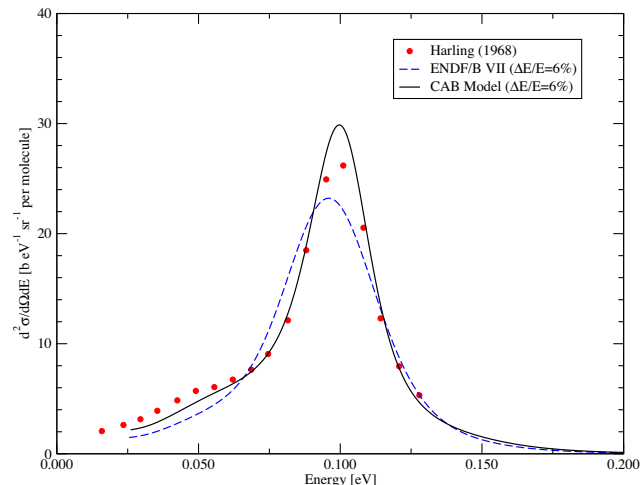


Fig. 9. Double differential scattering cross section for heavy water, $E_0 = 101$ meV, $\theta = 60^\circ$.

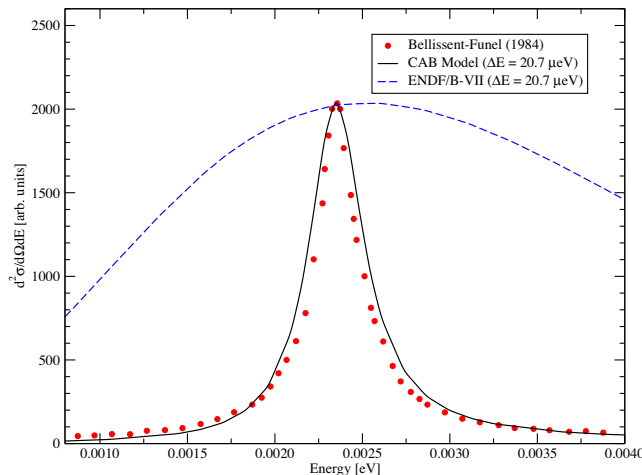


Fig. 10. Double differential scattering cross section for light water, $E_0 = 2.35$ meV, $\theta = 64.20^\circ$.

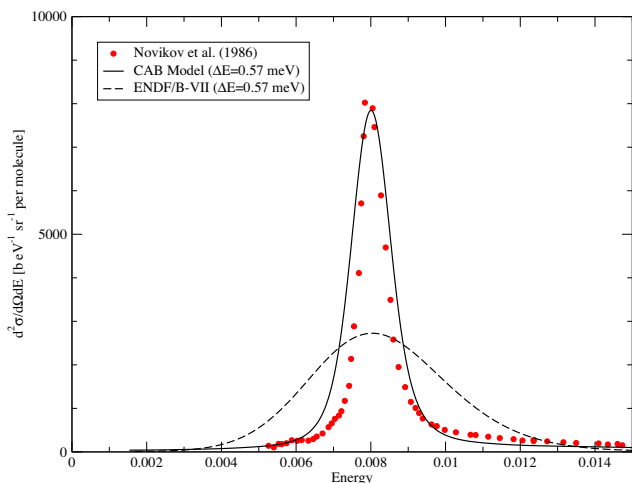


Fig. 8. Double differential scattering cross section for light water, $E_0 = 8$ meV, $\theta = 37^\circ$.

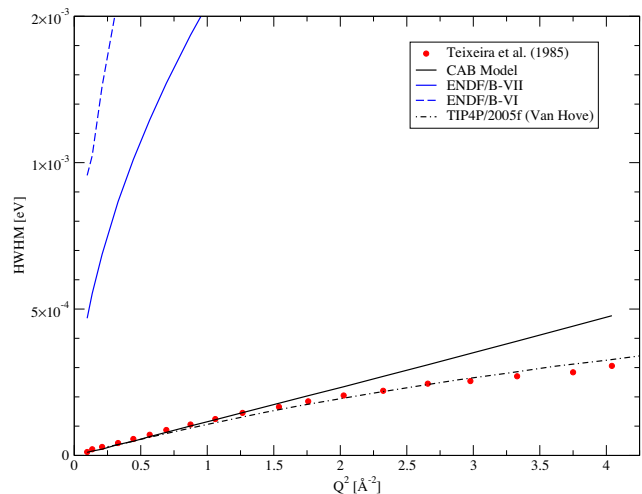


Fig. 11. Half-width of the quasielastic peak for $E_0 = 3.15$ meV neutrons in H_2O .

For heavy water, QENS calculations also show the effect of the Sköld correction used to obtain the coherent component. For a simple diffusion model, the HWHM is given by:

$$S_{\text{coh}}(Q, \omega) = \frac{1}{\pi} \frac{DQ^2/\tilde{S}(Q)}{\omega^2 + (DQ^2/\tilde{S}(Q))^2} \tilde{S}(Q)$$

$$S_{\text{coh}}(Q, \omega)|_{\text{max}} = S_{\text{coh}}(Q, 0) = \frac{1}{\pi} \frac{\tilde{S}^2(Q)}{DQ^2}$$

$$\text{HWHM} = \omega|_{S_{\text{coh}}(Q, \omega) = S_{\text{coh}}(Q, 0)/2}$$

$$\text{HWHM} = \frac{DQ^2}{\tilde{S}(Q)} \quad (18)$$

When we compare our calculations with the experimental results by Von Blanckenhagen (1972) (Fig. 12) we observe an oscillation (curve *b*) caused by the Sköld correction factor, around the DQ^2 behavior represented by the diffusion model (curve *c*). Again, if further improvement is needed in the quasielastic region, the scattering cross section could be computed directly from the Van Hove pair correlation functions (curves *d* and *e*).

5.3. Angular distribution

The coherent component of the scattering cross section manifest itself more clearly in the angular distribution of the cross section. The angular distribution of the cross section can be computed as:

$$\frac{d\sigma}{d\Omega} = \int_0^\infty dE' \left. \frac{d^2\sigma}{d\Omega E'} \right|_{\theta=\text{const}} \quad (19)$$

to be compared with experimental results.

In Figs. 13 and 14 we compare our calculations with measurements by Gibson (1978) and Walford (1980) of the angular distribution of neutrons with $E_0 = 327.4$ meV and $E_0 = 170$ meV in heavy water. The calculations computed with the ENDF/B-VI scattering law only reproduce the baseline because this library was computed on the incoherent approximation. The calculations computed with the ENDF/B-VII scattering law reproduce the first peak in the diffraction pattern but not the rest, because the structure factor that Keinert and Mattes used only included D–D structure. Overall, the agreement found with our model is better.

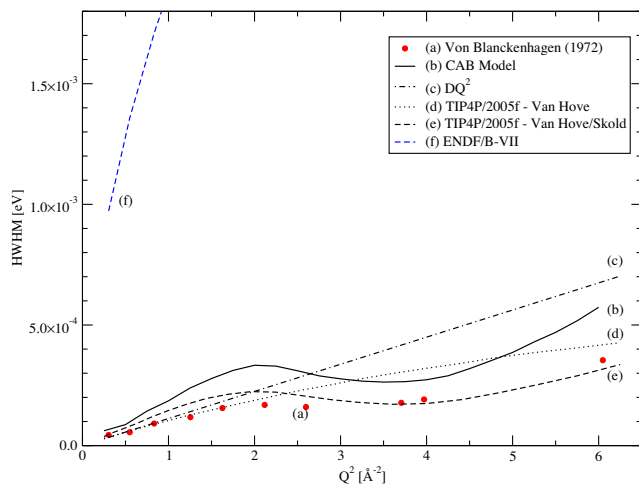


Fig. 12. Half-width of the quasielastic peak for $E = 5$ meV in D_2O .

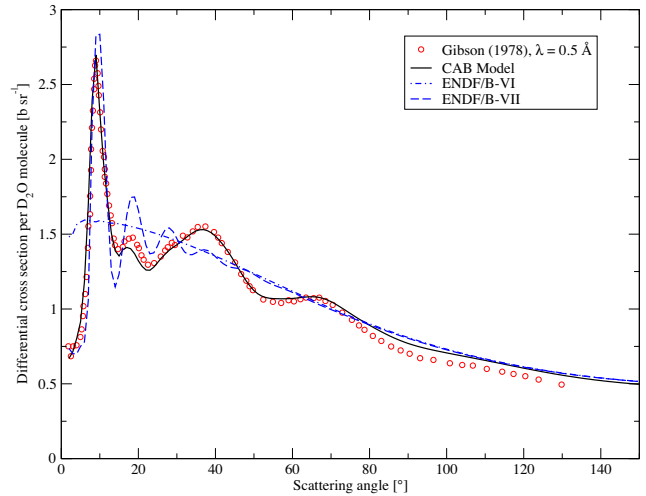


Fig. 13. Angular distribution for $E = 327.4$ meV in D_2O .

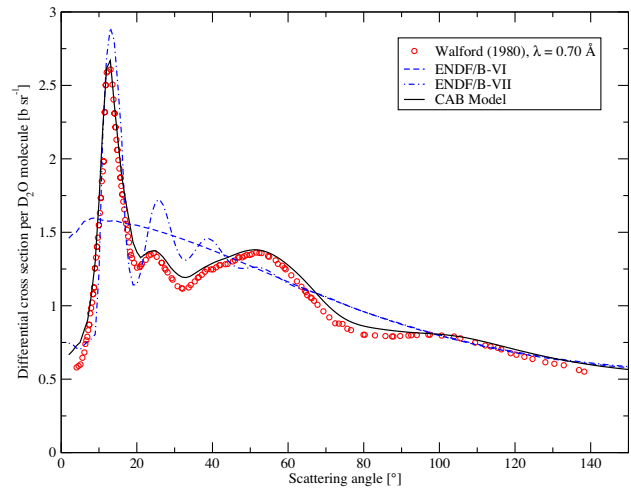


Fig. 14. Angular distribution for $E = 170$ meV in D_2O .

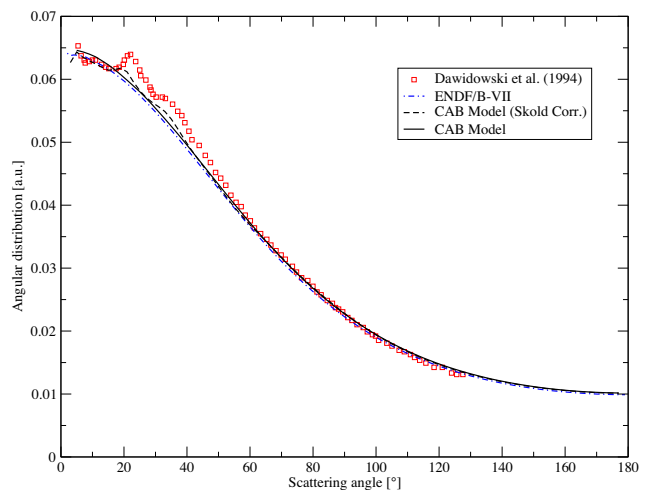


Fig. 15. Angular distribution for $E = 161.4$ meV in H_2O .

The comparison of the angular distribution for light water, compared with experimental results by Dawidowski et al. (1994) (Fig. 15) show good agreement, even in the incoherent approximation. If the slight diffraction pattern observed in the experimental results is important, the same Sköld correction used for heavy water can be applied to H and O in H₂O.

5.4. Average cosine of the scattering angle

The average cosine of the scattering angle can be computed by averaging the angular distribution for each incident energy:

$$\bar{\mu} = \frac{\int_{-1}^1 d\mu \mu \frac{d\sigma}{d\Omega}}{\int_{-1}^1 d\mu \frac{d\sigma}{d\Omega}} \quad (20)$$

In Fig. 16 we compare calculated results with our model and ENDF/B-VII for light water with measurements by Beyster et al. (1965). Overall, the results are similar to ENDF/B-VII.

When the diffusion model is used in LEAPR, convergence of the angular distribution requires the use of a fine α and β grid (see inset in Fig. 16).

For heavy water, our results compare well with the measurements by Beyster et al. (1965) (Fig. 17). Our model reproduces the low energy depression observed in the average scattering cosine calculations with ENDF/B-VII at ~2 meV, but also a second depression observed by Kornbichler (1965) at ~40 meV. As we will see in the total cross section, this second oscillation is associated with the effect of coherence in oxygen, which are not considered in the IKE model.

5.5. Total cross section

As a final test we compare the computed total cross sections for light water with measurements by Zaitsev et al. (1991) around room temperature (Fig. 18). Our model reproduces better the measured values of the total cross section in the cold neutron range, which are overpredicted by ENDF/B-VI and ENDF/B-VII by 60–100%.

For heavy water (Fig. 19), our model reduces the discrepancies found with the measurements by Kropff. Our model reproduces well the peak found at ~3 meV, but also the features observed around 20 meV range, which are caused by the coherent effects in the oxygen cross section.

To test the behavior of our model with temperature, we compared our calculations with the cold neutron measurements

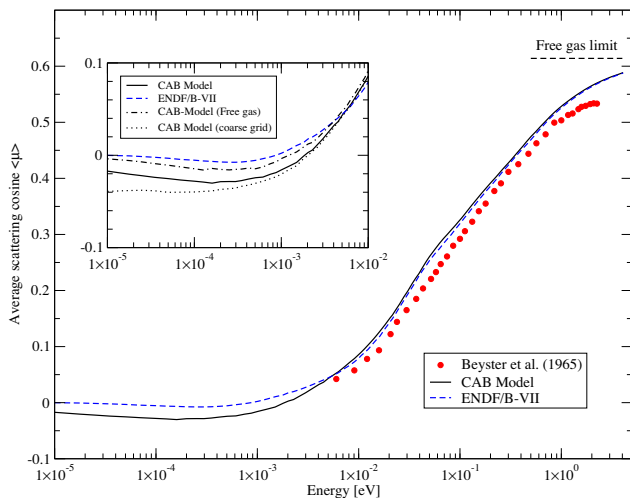


Fig. 16. Average cosine of the scattering angle for light water.

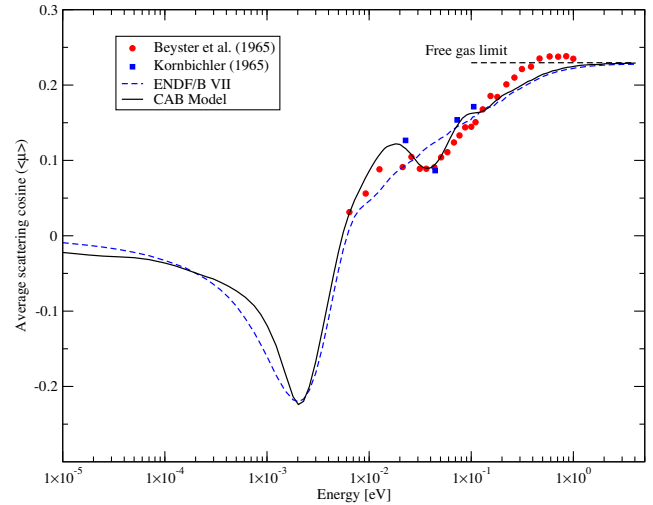


Fig. 17. Average cosine of the scattering angle for heavy water.

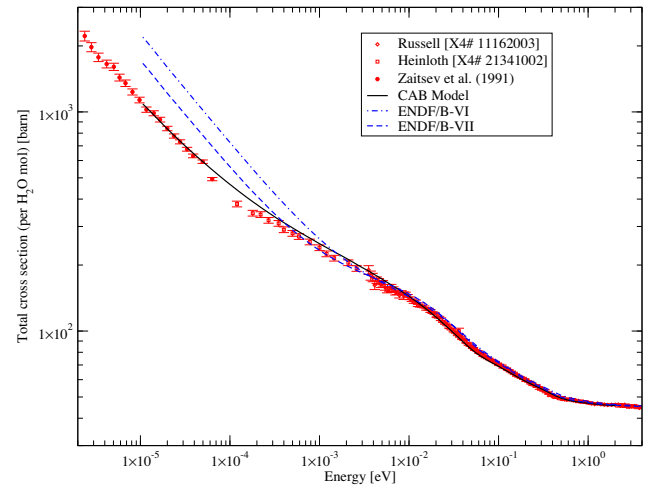


Fig. 18. Total neutron cross section for H₂O.

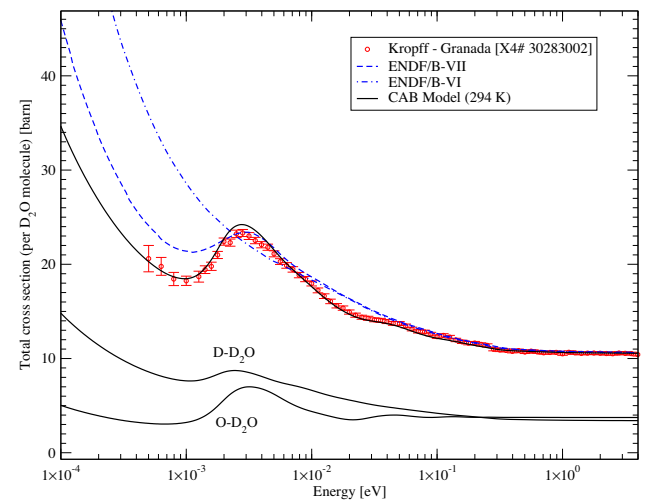


Fig. 19. Total neutron cross section for D₂O.

performed by Stepanov et al. (1974); Stepanov and Zhitarev (1976) at the IRT reactor of the Moscow Engineering Physics Institute. Stepanov published a series of measurements of the total

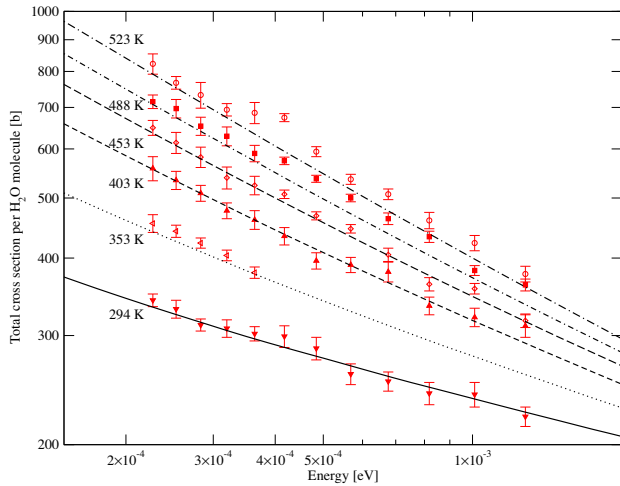


Fig. 20. Temperature dependence of the total neutron cross section for H_2O calculated with the CAB Model, compared with measurements by Stepanov.

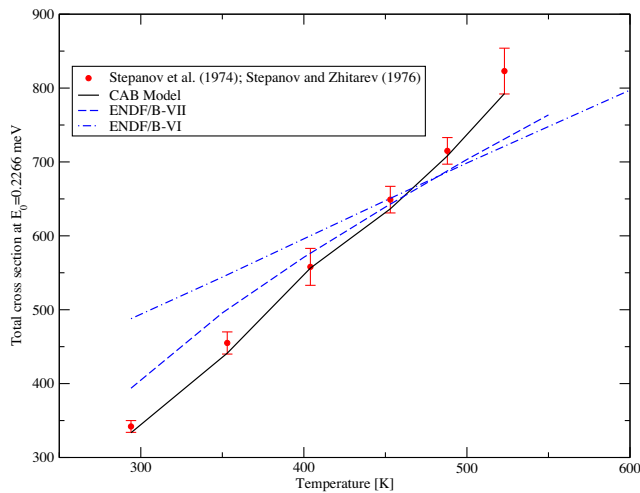


Fig. 21. Temperature dependence of the total neutron cross section for H_2O at $E_0 = 0.2266 \text{ meV}$.

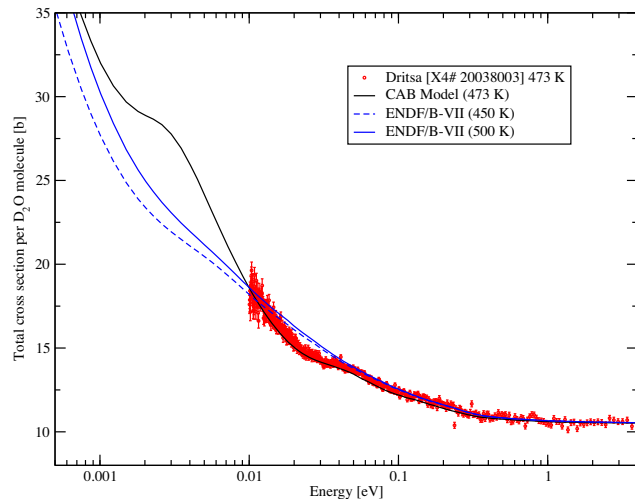


Fig. 22. Total neutron cross section for D_2O at 473 K.

cross section of liquid water at high temperatures for a fixed set of incident energies. In Fig. 20 we compare calculations with these measurements, finding good agreement. In Fig. 21 we compare

calculations with ENDF/B-VI, ENDF/B-VII and our model at the smallest incident energy available in the Stepanov data, $E_0 = 0.2266 \times 10^{-3} \text{ eV}$. As we can see, the use of a model that includes a detailed low energy dynamics allows us to reproduce better not only the values of the total cross section, but also its dependence with temperature.

In the case of heavy water, we compared our calculations with measurements by Dritsa (Fig. 22). Overall, the agreement with experimental data is better with our model.

6. Conclusions and future work

In this paper we presented a methodology to generate thermal scattering models for water, based on molecular dynamics simulations and experimental data. Using this methodology, we computed scattering law files in ENDF-6 format and thermal scattering cross sections for light water (H in H_2O) and heavy water (D and O in D_2O). This process was divided in two steps: the calculation of the generalized frequency spectrum from molecular dynamics simulations (which is discussed in more detail in reference Marquez Damian et al., 2013), and the generation of thermal scattering models from that spectrum. Although the molecular dynamics simulations contain an empirical water potential (TIP4P/2005f) that is adjusted to represent the dynamics and structure of water properly, once the generalized frequency spectrum is computed the evaluation of thermal scattering law files and generation of thermal neutron cross sections as presented in this paper does not entail the adjustment of free parameters, which leaves room for further optimization.

These models were produced within the approximations included in LEAPR/NJOY (the use of the Gaussian approximation to process the dynamics, and the use of the Egelstaff–Schofield diffusion model), which is the standard tool for this type of calculations, and approximations that are considered practical by the authors (namely, the calculation of light water in the incoherent approximation and the use of discrete oscillators to represent internal vibrations). When possible, we highlighted the limitations imposed by these approximations and hinted possible improvements for future work.

Measurable scattering quantities calculated using these models compare well with experimental values, and result in an improvement over existing scattering law files available from evaluated nuclear data libraries. In particular, the use of molecular diffusion produces a significant improvement in the cold neutron range in both light and heavy water, and the inclusion of measured structure factors results in a much better description of the angular distribution of scattered neutrons, total cross section and average scattering cosine in heavy water.

In this work we did not address the issue of covariances. There are current efforts to evaluate and propagate the covariance matrix in thermal scattering (Holmes and Hawari, 2012; Rochman and Koning, 2012) but to this day there is no established method to evaluate the covariance of the scattering law and the resulting covariance matrix cannot be stored in the current ENDF-6 format. That being said, the models presented in this paper are suitable to apply these perturbation methods currently under study; also, the differences found with existing models could be used to estimate the sensitivity of reactor calculations and other applications to thermal scattering data.

Acknowledgements

J.I. Márquez Damián acknowledges the support provided by CONICET. D.C. Malaspina acknowledges the support from NSF (Grant CHE-0957653).

References

- Abe, Y., Tsuboi, T., Tasaki, S., 2014. *Detectors and Associated Equipment* 735, 568.
- Bellissent-Funel, M.-C., Chen, S.H., Zanotti, J.M., 1995. *Physical Review E* 51, 4558.
- Bellissent-Funel, M.-C. et al., 1984. *Molecular Physics* 52, 1479.
- Beyster, J., Antunez, H., Brouwer, W., Carriveau, G., Crosbie, K., Koppel, J.U., Naliboff, Y.D., Neill, J.M., Russell Jr., J.L., Young, J.A., Young, J.C., 1965. Integral Neutron Thermalization – Annual Summary Report (GA-6824). General Atomics Technical Report.
- Bischoff, F., Bryant, W.A., Esch, L., Lajeunesse, C., Moore, W.E., Pan, S.S., Purohit, S.N., Yeater, M.L., 1967. Low Energy Neutron Inelastic Scattering (LENIS) in Linear Accelerator Project Progress Report RPI-328-27. (RPI Technical Report).
- Chadwick, M.B., Herman, M., Obložinský, P., Dunn, M.E., Danon, Y., Kahler, A.C., Smith, D.L., Pritychenko, B., Arbanas, G., Arcilla, R., et al., 2011. *Nuclear Data Sheets* 112, 2887.
- Dawidowski, J., Granada, J.R., Mayer, R.E., Cuello, G.J., Gillette, V., Bellissent-Funel, M.-C., 1994. *Physica B: Condensed Matter* 203, 116.
- Dore, J.C., 1985. *Water Science Reviews* 1, 3.
- Egelstaff, P., 1967. *An Introduction to the Liquid State*. Academic Press, London.
- Egelstaff, P., Schofield, P., 1962. *Nuclear Science and Engineering* 12, 260.
- Gibson, I.P., 1978. PhD. Thesis, U. of Kent.
- G Novikov, A., Lisichkin, Y.V., Fomichev, N.K., 1986. *Russian Journal of Physical Chemistry* 60, 1337.
- González, M.A., Abascal, J.L.F., 2011. *The Journal of Chemical Physics* 135, 224516.
- Harling, O.K., 1968. Slow-Neutron Inelastic Scattering and the Dynamics of Heavy Water. (BNWL Technical Report).
- Haywood, B., Page, D., 1968. Scattering Laws for Heavy Water at 540 K and Light Water at 550 K. In: *Proceedings of the Symposium on Neutron Thermalization and Reactor Spectra held at Ann Arbor, Michigan, IAEA*.
- Haywood, B., Thorson, I., 1962. The Scattering Law for Light and Heavy Water at 20 C and 150 C. In: *Proceedings of the Brookhaven Conference on Neutron Thermalization, IAEA*.
- Herman, M., Trkov, A., (Eds.), 2009. ENDF-6 Formats Manual. Report BNL-90365-2009, CSEWG Document ENDF-102. Brookhaven National Laboratory Technical Report.
- Holmes, J.C., Hawari, A., 2012. *Transactions of the American Nuclear Society* 107, 612.
- Keinert, J., Mattes, M., Sartori, E., 1984. JEF-1 scattering law data. JEF Report 2/JEF/DOC 41.2. Tec. Rep., IKE Stuttgart.
- Koppel, J., Houston, D., 1978. Reference manual for ENDF thermal neutron scattering data. GA-8774, ENDF-269. General Atomics Technical Report.
- Koppel, J., Young, J., 1965. *Nukleonik* 7, 408.
- Koppel, J., Triplett, J., Naliboff, Y., 1967. GASKET: A Unified Code for Thermal Neutron Scattering. GA-7417 (Rev.). General Atomics Technical Report.
- Kornbichler, S., 1965. *Nukleonik* 7, 281.
- Lappi, S.E., Smith, B., Franzen, S., 2004. *Spectrochimica Acta A* 60, 2611.
- MacFarlane, R.E., 1994. New thermal neutron scattering files for ENDF/B-VI release 2. LA-12639-MS. (LANL Technical Report).
- Marquez Damian, J.I., Granada, J.R., Dawidowski, J., Viñales, A.D. 2011. *Proceedings of AccApp '11 – Tenth International Topical Meeting on Nuclear Applications of Accelerators – Knoxville, TN ANS*.
- Marquez Damian, J.I., Malaspina, D.C., Granada, J.R., 2013. *The Journal of Chemical Physics* 139, 024504.
- Marti, J., Padro, J.A., Guardia, E., 1996. *The Journal of Chemical Physics* 105, 639.
- Mattes, M., Keinert, J., 2005. Thermal neutron scattering data for the moderator materials H₂O, D₂O and ZrHx in ENDF-6 format and as ACE library for MCNP (X) codes. INDC (NDS)-0470. (IAEA Technical Report).
- Mills, R., 1973. *The Journal of Physical Chemistry* 77, 685.
- Novikov, A.G., Vankov, A.A., Gosteva, L.S., 1990. *Journal of Structural Chemistry* 31, 77.
- Rahman, A., Stillinger, F., 1971. Molecular dynamics study of liquid water. *The Journal of Chemical Physics* 55, 3336.
- Rochman, D., Koning, A.J., 2012. *Nuclear Science and Engineering* 172, 278.
- Scopatz, A.M., Romano, P.K., Wilson, P.P.H., Huff, K.D., 2012. *Transactions of the American Nuclear Society* 107, 985.
- Soper, A.K., Benmore, C.J., 2008. *Physical Review Letters* 101, 65502.
- Stepanov, S.B., Zhitarev, V.E., 1976. *Atomic Energy* 41, 743.
- Stepanov, S.B., Zhitarev, V.E., Zelenyuk, F.M., Ya. Krasil'nikov, V., 1974. *Atomic Energy* 37, 1094.
- Teixeira, J., Bellissent-Funel, M.C., Chen, S.H., Dianoux, A.J., 1985. *Physical Review A* 31, 1913.
- Van Der Spoel, D., Lindahl, E., Hess, B., Groenhof, G., Mark, A.E., Berendsen, H.J.C., 2005. *Journal of Computational Chemistry* 26, 1701.
- Viñales, A.D., Dawidowski, J., Marquez Damian, J.I., 2011. *Annals of Nuclear Energy* 8, 1687.
- Vineyard, G.H., 1958. *Physical Review* 110, 999.
- Von Blanckenhagen, P., 1972. *Berichte der Bunsen-Gesellschaft-Physical Chemistry Chemical Physics* 76, 891.
- Walford, G., 1980. PhD. Thesis, U. of Kent.
- Walford, G., Clarke, J.H., Dore, J.C., 1977. *Molecular Physics* 33, 25.
- Yoshida, K., Wakai, C., Matubayasi, N., Nakahara, M., 2005. *The Journal of Chemical Physics* 123, 164506.
- Zaitsev, K., Petrov, V., Kuznetsov, S., Langer, O., Meshkov, I., Perekrestenko, A., 1991. *Atomic Energy* 70, 238.